Developmental Biology 414 (2016) 108–120

Contents lists available at ScienceDirect

Developmental Biology

journal homepage: www.elsevier.com/locate/developmentalbiology

Evolution of developmental control mechanisms

Glypican1/2/4/6 and sulfated glycosaminoglycans regulate the patterning of the primary body axis in the cnidarian *Nematostella vectensis*

Markus Bause, Roddy van der Horst, Fabian Rentzsch *

Sars Centre for Marine Molecular Biology, University of Bergen, Thormøhlensgt 55, 5008 Bergen, Norway

ARTICLE INFO

Article history:
Received 14 November 2015
Received in revised form
22 March 2016
Accepted 13 April 2016
Available online 14 April 2016

Keywords:
Glycoproteins
Proteoglycans
HSPGs
Wnt-pathway
FGF
Anterior-posterior axis
Apical sensory organ
Apical tuft
Endosulfatase
Frizzled5/8

ABSTRACT

Glypicans are members of the heparan sulfate (HS) subfamily of proteoglycans that can function in cell adhesion, cell crosstalk and as modulators of the major developmental signalling pathways in bilaterians. The evolutionary origin of these multiple functions is not well understood. In this study we investigate the role of glypicans in the embryonic and larval development of the sea anemone *Nematostella vectensis*, a member of the non-bilaterian clade Cnidaria. *Nematostella* has two *glypican* (*gpc*) genes that are expressed in mutually exclusive ectodermal domains, *NvGpc1/2/4/6* in a broad aboral domain, and *NvGpc3/5* in narrow oral territory. The endosulfatase *NvSulf* (an extracellular modifier of HS chains) is expressed in a broad oral domain, partially overlapping with both *glypicans*. Morpholino-mediated knockdown of *NvGpc1/2/4/6* leads to an expansion of the expression domains of aboral marker genes and a reduction of oral markers at gastrula stage, strikingly similar to knockdown of the Wnt receptor *NvFrizzled5/8*. We further show that treatment with sodium chlorate, an inhibitor of glycosaminoglycan (GAG) sulfation, phenocopies knockdown of *NvGpc1/2/4/6* at gastrula stage. At planula stage, knockdown of *NvGpc1/2/4/6* and sodium chlorate treatment result in alterations in aboral marker gene expression that suggest additional roles in the fine-tuning of patterning within the aboral domain. These results reveal a role for *NvGpc1/2/4/6* and sulfated GAGs in the patterning of the primary body axis in *Nematostella* and suggest an ancient function in regulating Frizzled-mediated Wnt signalling.

1. Introduction

The patterning of the anterior-posterior (A-P) body axis is a fundamental step in animal embryogenesis. In bilaterians, several conserved molecular systems have been identified that regulate the development of particular regions along the A-P axis. Wnt/β-catenin signalling specifies the site of gastrulation; this is considered to be the posterior pole. The expression of Wnts at the gastrulation site can then establish graded Wnt/β-catenin signalling activity and provide positional information with maximal levels at the posterior pole (Martin and Kimelman, 2009; Niehrs, 2010; Petersen and Reddien, 2009). *Hox* genes determine the identity of consecutive domains along the A-P axis (Akam et al., 1994; Gellon and McGinnis, 1998; Krumlauf, 1994; Mallo et al., 2010) except for the anterior-most regions, which develop under the control of several transcription factors with *six3* as a key regulator of the anterior patterning program (Lagutin et al., 2003; Posnien et al., 2011; Steinmetz et al., 2010; Wei et al., 2009). While the molecular basis of A-P patterning has been studied in detail in some bilaterian model organisms, the early evolution of axial patterning mechanisms is less well understood. Cnidarians are the sister group of bilaterians (Hejnol et al., 2009; Philippe et al., 2011, 2009; Ryan et al., 2013) and thus occupy an important phylogenetic position for comparative studies on embryonic development. Here we use the sea anemone *Nematostella vectensis* to analyse the molecular regulation of the patterning of the primary body axis in a non-bilaterian model system.

Nematostella embryogenesis encompasses a hollow blastula stage, gastrulation by invagination and the formation of a free-swimming planula larva before the animals become sessile polyps with a single body opening that is surrounded by a ring of tentacles (Hand and Uhlinger, 1992; Kraus and Technau, 2006; Magie et al., 2007). Gastrulation occurs in the domain that is derived from the animal pole of the oocyte and the blastopore becomes the single body opening (Fritzenwanker et al., 2007; Lee et al., 2007). This opening is traditionally described as oral, despite its three functions for the ingestion and egestion of food and as a gonopore. As in bilaterians, Wnt/β-catenin signalling is a key regulator of the patterning of the oral-aboral

* Corresponding author.
E-mail address: fabian.rentzsch@uib.no (F. Rentzsch).

http://dx.doi.org/10.1016/j.ydbio.2016.04.011

axis (Kumburegama et al., 2011; Kusserow et al., 2005; Leclère et al., 2016; Marlow et al., 2013; Röttinger et al., 2012; Sinigaglia et al., 2013; Wikramanayake et al., 2003). While gastrulation and endoderm formation occur at the site of high NvWnt/Nvβ-catenin signalling at the future oral pole (Lee et al., 2007; Wikramanayake et al., 2003), Nvβ-catenin is in addition required for establishing a regulatory system in the aboral half of the blastula, with *NvSix3/6* acting as a key positive regulator of aboral domain development (Leclère et al., 2016; Sinigaglia et al., 2013). Importantly, the Wnt receptor *NvFrizzled 5/8* (*NvFz5/8*) is expressed in the aboral domain from mid-blastula stage on, and serves to restrict the size of the aboral domain by negatively regulating *NvSix3/6* (Kumburegama et al., 2011; Leclère et al., 2016; Sinigaglia et al., 2015). The expression patterns of *Hox* genes do not suggest that they act in a bilaterian-like manner to determine the identity of adjacent territories along the oral-aboral axis (Finnerty et al., 2004; Layden et al., 2016; Manuel, 2009; Ryan and Baxevanis, 2007). After gastrulation, a long ciliary tuft develops at the aboral pole. This is believed to be part of a larval sense organ, the apical organ (Richter et al., 2010) although no functional or developmental connection to the nervous system has been shown yet in *Nematostella* (Marlow et al., 2014; Nakanishi et al., 2012; Richards and Rentzsch, 2014). The development of the apical organ is under the control of two Fibroblast Growth Factors (FGFs) with opposing functions: Signalling by NvFGFa1 via the FGF receptor NvFGFRa is required for the formation of the apical organ, whereas NvFGFa2 functions to limit its size (Rentzsch et al., 2008). Thus, Wnt and FGF signalling play prominent roles in the development of the aboral domain of *Nematostella* and these observations prompted us to analyse the function of potential co-regulators of these pathways, the glypicans.

Glypicans are extracellular proteoglycans that are connected to the cell membrane via a GPI (glycosylphosphatidylinositol) anchor. Proteoglycans are molecules in which one or more glycosaminoglycans (GAGs, long unbranched sugar chains consisting of disaccharide repeats) are covalently linked to a core protein (Esko et al., 2009). The GAG that is linked to glypicans is heparan sulfate and accordingly glypicans belong to the heparan sulfate subfamily of proteoglycans (HSPGs, Sarrazin et al., 2011). In bilaterians, glypicans regulate several developmental processes by their ability to modulate the activity of the Wnt, Hedgehog, BMP and FGF signal transduction pathways (Bishop et al., 2007; Fico et al., 2011; Filmus et al., 2008; Hacker et al., 2005; Lin, 2004). While in some cases the binding of the glypican core proteins to signalling ligands is required for their function (Kirkpatrick et al., 2006; Yan et al., 2009), the developmental roles of glypicans in most cases depend on the interaction of the heparan sulfate (HS) chains with ligands and/or receptors (e.g. Fico et al., 2011).

The covalent linkage of HS chains to the core protein and HS chain elongation occur in the Golgi. The growing HS chains are subject to several modifications, most prominently N-and O-sulfation, which are carried out by NDSTs (N-deacetylase/N-sulfotransferases) and HS-OSTs (HS O-sulfotransferases), respectively. O-sulfation can occur at different positions in the sugar molecules and is catalyzed by position-specific enzymes (HS2OST, HS3OST and HS6OST; reviewed in: Bulow and Hobert (2006) and Esko and Selleck (2002)). Sulfs (6-O endosulfatases) are unique among the HS modifying enzymes in that they also act in the extracellular space to remove sulfation (a modification that cannot be reversed by the only Golgi-localized HS-6OST) (Ai et al., 2003). Different studies have shown that the sulfation or desulfation of HS (by HS-OSTs and Sulfs, respectively) significantly affect the specificity of ligand binding in both the FGF and the Wnt pathways in a cell autonomous manner (Ai et al., 2003; Dhoot et al., 2001; Kleinschmit et al., 2013; Venero Galanternik et al., 2015; Wang et al., 2004).

Several mechanisms have been described by which glypicans can affect the activity of signalling molecules, including the promotion of ligand-receptor interactions, the sequestration of ligands and the enhanced or reduced mobility of ligands in the extracellular space. These mechanisms and their net effects on signalling activity can differ for individual glypican-ligand combinations and between different tissues or cell types (Fico et al., 2011; Matsuo and Kimura-Yoshida, 2013, 2014; Sarrazin et al., 2011; Yan et al., 2009). The variety of these interactions, including cell autonomous and long-range types of fine-tuning, enable glypicans to be multifaceted modulators of signalling pathways.

A previous study showed that the enzymes required for HS biosynthesis and modifications are present in *Nematostella* and that the HS chains in these animals have an unusual disaccharide composition (Feta et al., 2009). Here we show that *NvGlypican1/2/4/6* (*NvGpc1/2/4/6*) and the sulfation of HS chains are involved in the patterning of the oral-aboral axis and the proper development of the apical organ of *Nematostella*.

2. Materials and methods

2.1. Nematostella culture

Animals were maintained in 1/3 filtered seawater (*Nematostella* medium (NM)) and induced to spawn as described previously (Fritzenwanker and Technau, 2002). Fertilised egg packages were incubated in 3% cysteine/NM for 25 min on a rotary shaker to dissolve the jelly mass surrounding the eggs. Embryos were raised at 21 °C until 24 hpf (hours post-fertilisation) for gastrula stages, 48 hpf for mid-planula, and 72 hpf for late planula stages.

2.2. Identification of the sequences

Gene models for *NvGlypican1/2/4/6* and *NvGlypican3/5* (protein ID 247677 and 134347, respectively at http://genome.jgi.doe.gov/Nemve1/Nemve1.home.html) were used to design RACE (Rapid Amplification of CDNA Ends) primers. Standard methods for 3′ and 5′RACE were carried out with cDNA templates from mixed *Nematostella vectensis* developmental stages (SMARTer™ RACE cDNA Amplification Kit, Clontech Laboratories, Mountain View, CA, USA) The obtained full length sequences were cloned into pGemT vector (Promega, Madison, WI, USA) and sequenced.

2.3. Phylogeny

We used the MEGA6 software to align selected sequences and to carry out phylogenetic analyses, as described (Hall, 2013). The region selected for the alignment was the conserved glypican domain of ca. 390 amino acids, which contains 14 cysteine residues (Fico et al., 2011). We used Maximum Likelihood analysis with a LG+G+I model with partial deletion for all trees shown. Robustness was tested using the bootstrap method with 500 replicates. We used glypican orthologues of the following species for our analysis: Aq (*Amphimedon queenslandica*); Dm (*Drosophila melanogaster*); Hm (*Hydra magnipapillata*); Hs (*Homo sapiens*); Nv (*Nematostella vectensis*) Rn (*Rattus norvegicus*); Sp (*Strongylocentrotus purpuratus*. Accession numbers: AqGpcA: XP_003386976; AqGpcB: XP_003386974; DmDallyLike: AAS65005.1; DmDally: AAA97401.1; HmGpc4like: XP_002157574; HsGpc1: AAH51279.1; HsGpc2: AAH27972.1; HsGpc3: AAH35972.1; HsGpc4: AAH17166.1; HsGpc5: AAH39730.1; HsGpc6: CAC21820.2; RnGpc1: AAA41251.1; RnGpc2: NP 612520.1; RnGpc3: AAH85756.1; RnGpc4: AAH81962.1; RnGpc5: NP 1100755.2; RnGpc6: EDM02516.1; SpGpc5: NP 1138966.1; SpGpc6: NP 1138965.1.

2.4. In situ hybridisation (ISH) and Immunohistochemistry (IHC)

Due to a developmental delay of approximately 2 h in embryos that undergo injection, the following fixation times were used for achieving comparable gastrula stage embryos across experiments. Injected: 26 hpf. WT/drug treated: 24 hpf. IHC experiments were carried out as described in Nakanishi et al. (2012) and Sinigaglia et al. (2013). ISH was carried out as following: Embryos were fixed for 90 s in ice cold 0.25% glutaraldehyde + 3.7% formaldehyde in *Nematostella* Medium, followed by 1 h in 3.7% formaldehyde in PBT (PBS + 0.1%Tween20) at 4 °C. After 4 washes in PBT, and one in deionized water, embryos were stored at −20 °C in MeOH. Animals were rehydrated in a PBT-MeOH dilution series and washed in PBT (3 ×). After proteinase K treatment (20 μg/ml for 10 min), they were washed twice in 4 mg/ml glycine in PBT, then 3 × in 0.1 M TEA pH7.8, with 0, 0.25% and 0.5% acetic anhydride, respectively. After 3 washes in PBT the samples were refixed in 3.7% formaldehyde in PBT for 30 min and washed five times in PBT. Prehybridization was at 60 °C for at least 2 h in Hybridization solution made with 50% formamide, 5 × SSC, 1% SDS, 0.1% Tween20, 50 μg/ml heparin, 100 μg/ml salmon sperm DNA, 9 mM citric acid; Hybridisation at 60 °C lasted for at least 60 h. In 30 min washes hybridisation solution was substituted in a dilution series by 25%, 50%, 75%, 100% SSCT at 60 °C and subsequently by PBT at RT. After > 2 h of blocking in 1% Boehringer Blocking Solution in Maleic acid buffer (100 mM maleic acid, 150 mM NaCl, pH7.5), animals were incubated with anti-DIG-AP antibody (Roche) 1:4000 in blocking solution at 4 °C overnight. Excess antibody was removed by 10 × 15 min washes in PBT + 0.2% TritonX100 + 0.1%BSA. After equilibration in NTMT (100 mM Tris pH9.5; 100 mM NaCl; 50 mM $MgCl_2$; 0.1% Tween 20) buffer, staining with NBT/BCiP (Roche) in NTMT was carried out at RT. Imaging was conducted on a Nikon Eclipse E800 compound microscope with a Nikon Digital Sight DSU3 camera for ISH, or on a Leica SP5 confocal microscope for IHC. Figure plates were built using Adobe photoshop CS5 and Adobe Illustrator CS6; images were cropped and adjusted for brightness/contrast and colour balance; any adjustments were always applied to the whole image.

2.5. Morpholino injection

Microinjections were carried out as described in (Rentzsch et al., 2008). Fertilised eggs were injected with 250–750 μM morpholino (GeneTools), 50 ng/μl Alexa Fluor conjugated Dextran (Invitrogen) in nuclease free water. For control injections we used a five mismatch (mm) control morpholino; mismatch nucleotides shown in lower case, ATG is underlined:

*NvGpc1/2/4/6*ATGmm: 5′-AAATCgAAcCTATTgTGTaCcCCAT-3′.

*NvGpc1/2/4/6*ATGMO: 5′-AAATCCAAGCTATTCTGTTCGCCAT-3′.

*NvFz5/8*MO: 5′-CCCGATCAAGTCTTCGAGTAGCCAT-3′ (Leclère et al., 2016).

*NvFGFa1*MO: 5′-ATAAGGTGGACGCATGACTTTGTAG-3′ (Rentzsch et al., 2008).

*NvFGFa2*MO: 5′-CGTTAGCATGGTGATCGTCATGTTG-3′ (Rentzsch et al., 2008).

Morpholino binding was tested by cloning the *NvGpc1/2/4/6*MO target-site in front of EGFP in the pCS2 + vector. Capped mRNA was synthesised in vitro using the mMessage mMACHINE SP6 Transcription Kit (Ambion) and purified using the MEGAclear Transcription Clean-up Kit (Ambion). mRNAs (40 ng/μl) encoding EGFP or *NvGpc1/2/4/6*MOtarget-site-EGFP were co-injected with either the gene-specific or control morpholino (300 μM), and Alexa568-coupled Dextran (40 ng/μl). EGFP expression was examined at 24 hpf; images of all conditions were captured using identical acquisition settings.

2.6. RT-qPCR

RNA from embryos from 3 independent injections was extracted using the RNAqueous kit (Ambion), and DNAase treated using TurboDNase (Ambion). Quality and quantity of RNA was assessed using a Bioanalyzer (Agilent). cDNA was reverse transcribed using Superscript III (Invitrogen) primed with random hexamers (Roche). RT^- control reactions (without reverse transcriptase) were prepared for all samples. Primer pairs with PCR efficiencies of 95–106% were used for RT-qPCR. 2 technical replicates were performed for each of the 3 biological replicates. Relative expression was calculated using the delta-delta-ct method; control gene stabilities were assessed using RefFinder (http://fulxie.0fees.us/?type=reference), with *NvATP-synthase* and *NvELF1B* being selected as most stable. Mean relative expression and standard error of 3 biological replicates is plotted. For primer sequences see Table S1.

2.7. Sodium chlorate and azakenpaullone treatment

Animals were treated with sodium chlorate ($NaClO_3$) with concentrations ranging from 10 to 200 mM in *Nematostella* medium from 6.5 hpf until 24 hpf (gastrula stage) or 72 hpf (planula stage), from 24 hpf to 72 hpf, from 48 hpf to 72 hpf and from 24 hpf to 72 hpf. See also scheme in Fig. 10.

1-Azakenpaullone (CalBiochem #191500) was dissolved to a concentration of 10 mM in DMSO, this stock was diluted in *Nematostella* medium to 1 μM. Embryos were treated from 6.5 to 26 hpf. Control animals were treated with the same concentration of DMSO.

3. Results

3.1. The two major groups of glypicans (1/2/4/6 and 3/5) were already present in the earliest metazoans

There are two *glypican* genes in the *Nematostella* genome (Matus et al., 2008). Phylogenetic analysis places one of these genes within the *glypican 3/5* family (*NvGpc3/5*). The other gene (*NvGpc1/2/4/6*) clusters with *Drosophila Dally-like*, and is likely a member of the *glypican1/2/4/6* family (Fig. 1). Glypican genes from the sponges *Amphimedon queenslandica* and *Sycon ciliatum*, the placozoan *Trichoplax adhaerens* and the ctenophores *Mnemiopsis leidyi* and *Pleurobrachia bachei* did not fall into one of these subgroups in our analysis (Figs. 1 and S1). Invertebrate genomes typically contain two glypicans, whereas many vertebrates have six (or more in fish) *glypican* genes, likely due to single gene and whole genome duplications. In mammals, *glypican 3* and *4*, and *glypican 5* and *6*, respectively, are closely linked in the genome (Filmus et al., 2008). Similarly, the two *Nematostella glypican* genes are neighbours in the genome, with only 5456 bp between the stop codon of *NvGpc3/5* and the start codon of *NvGpc1/2/4/6*. This indicates that the last common ancestor of cnidarians and bilaterians likely had two *glypican* genes in close vicinity in the genome (as previously assumed (Filmus et al., 2008)).

Both predicted *Nematostella* glypicans contain 14 cysteine residues whose conserved spacing pattern is thought to contribute to the folding into a globular domain (Bernfield et al., 1999; Veugelers et al., 1999). Near the C-terminus, both NvGpc1/2/4/6 and NvGpc3/5 have several serine-glycine dipeptides, which likely function as GAG attachment sites (Esko and Zhang, 1996; Zhang et al., 1995).

3.2. The two Nematostella glypicans are expressed in opposing patterns

In situ hybridisation (ISH) revealed distinct expression domains for both *Nematostella glypican* genes during development. *NvGpc1/*

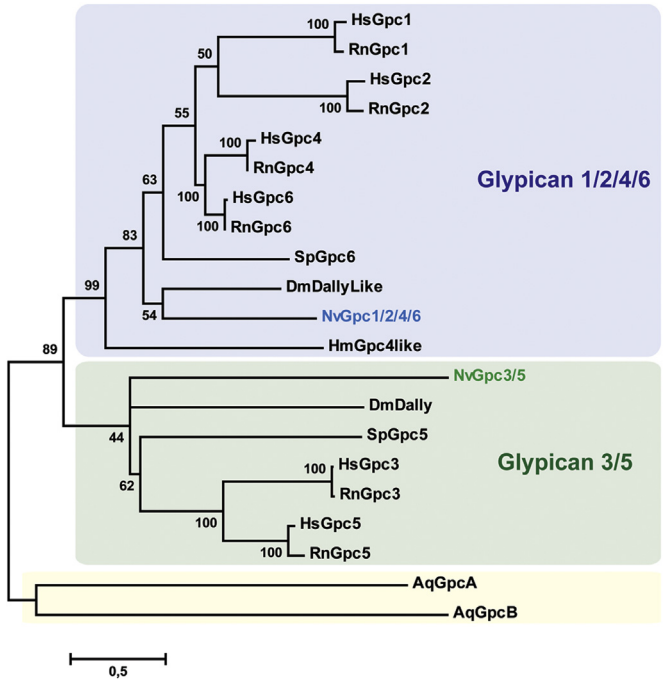

Fig. 1. The two *Nematostella vectensis* glypican orthologs group with the two major glypican subfamilies Gpc1/2/4/6 and Gpc3/5. Unrooted phylogenetic tree of selected glypicans. The Maximum Likelihood method was used within the MEGA6 software to estimate the tree. The LG+G+I model with partial deletion was used and robustness was tested using the bootstrap method with 500 replicates; values are indicated next to the branches. The two *Nematostella* glypicans cluster with the Gpc1/2/4/6 and Gpc3/5 subgroups, whereas glypicans from the sponge *Amphimedon queenslandica* and other non-bilaterians do not fall into one of the two subgroups (see also Fig. S1). For accession numbers and further details see materials and methods. Aq (*Amphimedon queenslandica*); Dm (*Drosophila melanogaster*); Hm (*Hydra magnipapillata)*; Hs (*Homo sapiens*); Nv (*Nematostella vectensis*) Rn (*Rattus norvegicus*); Sp (*Strongylocentrotus purpuratus*). The blue box indicates the Glypican 1/2/4/6 group, the green box the Glypican3/5 group. Sequences in the yellow box do not fall into the two known subgroups.

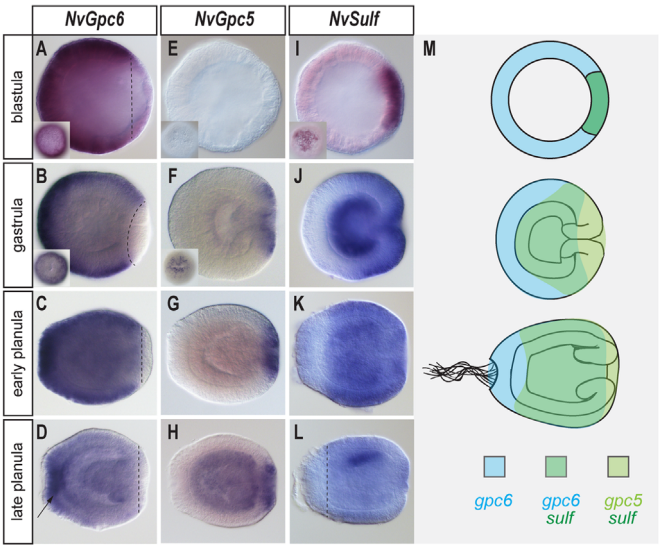

Fig. 2. *NvGpc3/5* and *NvGpc1/2/4/6* are expressed in distinct, opposing regions along the oral-aboral axis. (A–L) Lateral views of in situ hybridisations with aboral pole to the left, insets are oral views, stages are indicated to the left, probes on top. **(A–D)** *NvGpc1/2/4/6* is expressed throughout the ectoderm; only the oral region is free of expression (dotted line), at later stages expression is stronger in the region of the apical organ (arrow in **D**). **(E–H)** *NvGpc3/5* is expressed early in the putative oral territory, then later also in the endoderm. **(I–L)** *sulf* is expressed throughout the ectoderm and endoderm of developing larvae, only the aboral pole (in the ectoderm and at planula stage also the most aboral endoderm) are free of expression. **(M)** Three territories along the oral-aboral axis are formed by the combined expression of these three genes in gastrula and planula stage. Note that *NvGpc5* corresponds to *NvGpc3/5*, and *NvGpc6* to *NvGpc1/2/4/6* in all figures.

2/4/6 is first broadly expressed in the ectoderm, except for the oral-most region, which is free of expression from mid-blastula (12 hpf) stage on (Fig. 2A, note that in all figures, NvGpc1/2/4/6 is labelled as NvGpc6 and NvGpc3/5 as NvGpc5). At gastrula stage, *NvGpc1/2/4/6* expression is found throughout the ectoderm, still with the exception of the oral part and now at higher levels in the aboral domain (Fig. 2B). This pattern is also observed in planula stages, with the elevated aboral expression more restricted to the region of the apical organ (Fig. 2C and D). This expression pattern resembles that of *NvFGFRa* (Matus et al., 2007) and also encompasses the expression domain of the Wnt-receptor *NvFz5/8* (Kumburegama et al., 2011; Leclère et al., 2016; Sinigaglia et al., 2015).

NvGpc3/5 expression is not detectable by ISH at mid-blastula (Fig. 2E). At late blastula stage (16 hpf), expression commences on one side of the embryo (data not shown) and at gastrula and early planula stages it is expressed in a small domain around the blastopore (Fig. 2F and G). At late planula stage *NvGpc3/5* is also expressed uniformly in the endoderm (Fig. 2H). Since regulation of the HS sulfation status by the 6-O endosulfatase *Sulf* has been shown to affect the interaction of HSPGs with signalling molecules (see introduction) we re-assessed the expression pattern of *NvSulf*. Previously, we had shown that *NvSulf* is expressed in the endoderm from gastrula stage on (Feta et al., 2009). Using an improved ISH protocol (see Material and Methods) we have now refined this observation. *NvSulf* expression starts between 12 and 14 hpf on one side of the blastula (Fig. 2I), which is, based on the staining at later stages, presumably the future oral domain (morphologically it is not possible to identify the oral-aboral axis at this stage). At gastrula stage *NvSulf* is expressed throughout the endoderm and in the entire oral hemisphere of the ectoderm (Fig. 2J). At planula stage, only in the aboral pole of the ectoderm (encompassing approximately 25% of the ectoderm along the oral-aboral axis) and in the most aboral endoderm, *NvSulf* expression cannot be detected (Fig. 2K and L). At late planula stage, elevated levels of *NvSulf* transcripts are observed on one side of the endoderm (Fig. 2L). Thus, the expression patterns of the *NvGpcs* and *NvSulf* demarcate three territories along the oral-aboral axis in *Nematostella* larvae (Fig. 2M): the oral territory where *NvGpc3/5* is co-expressed with *NvSulf*; the midbody territory with co-expression of *NvGpc1/2/4/6* and *NvSulf*, and the aboral territory, where *NvGpc1/2/4/6* is co-expressed with *NvFz5/8* and *NvFGFRa*.

Since we are particularly interested in the development of the aboral domain, we focused subsequent functional analyses on *NvGpc1/2/4/6*.

3.3. *NvGpc1/2/4/6 knockdown leads to a shift in expression domains along the oral-aboral axis*

We investigated the function of *NvGlypican1/2/4/6* during embryonic development by injection of a translation blocking morpholino (*NvGpc1/2/4/6* MO, labelled as *NvGpc6* MO in the figures). We tested the *NvGpc1/2/4/6* MO activity by co-injecting it with mRNA in which the *NvGpc1/2/4/6* MO target site was placed upstream of EGFP. The *NvGpc1/2/4/6* morpholino blocked the translation of the *EGFP* mRNA that contained the target site, but not of the *EGFP* mRNA lacking the MO target site; a corresponding five mismatch control MO did not block translation from the *EGFP* mRNA containing the target site (Fig. S2).

At gastrula stage, we observed a shift of the expression patterns of regional marker genes along the oral-aboral axis towards the oral pole in *NvGpc1/2/4/6* knockdown animals. In control morpholino injected animals, as in wildtype (WT) animals, *NvFGFa2* marks the aboral pole

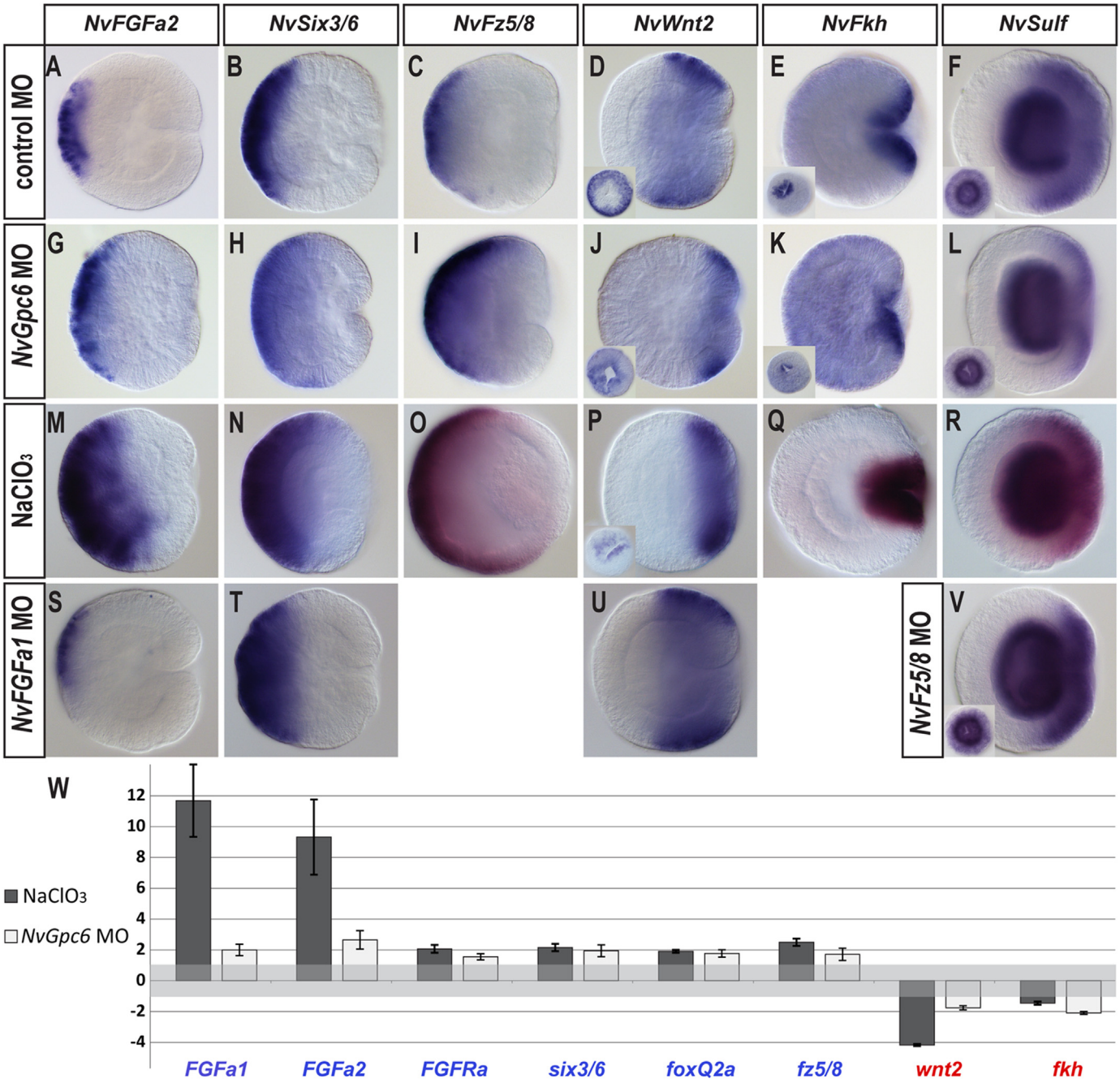

Fig. 3. Injection of *NvGpc1/2/4/6* morpholino and $NaClO_3$ treatment result in aboralisation at gastrula stage. (A–V) Lateral views of in situ hybridisations with aboral pole to the left, insets are oral views, all animals are at mid-gastrula stage. Treatments or morpholinos are indicated on the left, probes on top. Control MO injected animals **(A–F)** show WT expression (see text for WT-expression references). *NvGpc1/2/4/6* knockdown animals **(G–L)** and $NaClO_3$ treated animals **(M–R)** phenocopy a *NvFz5/8* knockdown (**V** and Leclère et al., 2016): Animals show shifted expression patterns along the oral-aboral axis, towards the oral pole at gastrula stage – i.e. aboralisation. *NvFGFa1* knockdown leads to the downregulation of *NvFGFa2* **(S)** while other markers remain unchanged (**T** and **U**). **(W)** RT-qPCR confirms the upregulation of aborally expressed genes (blue) and the downregulation of orally expressed genes (red) in *NvGpc1/2/4/6* knockdown and $NaClO_3$ treated animals. Graph shows fold changes of morpholino injected animals compared with animals injected with a *NvGpc1/2/4/6* mismatch MO (white boxes); and $NaClO_3$ treated vs. untreated animals (grey boxes). ± 1 means no change (shaded grey), $+2$ is 100% upregulation (see Section 2 for details).

(Rentzsch et al., 2008), *NvSix3/6* and *NvFz5/8* expression covers approximately a third of the gastrula on the same, aboral side as *NvFGFa2* (Kumburegama et al., 2011; Sinigaglia et al., 2013), *NvWnt2* is expressed adjacent to this domain more orally (Kusserow et al., 2005) and *NvFkh* marks the oral opening and the pharynx (Fritzenwanker et al., 2004; Martindale et al., 2004) (Fig. 3A–E). Upon *NvGpc1/2/4/6* knockdown the expression domains of *NvFGFa2*, *NvSix3/6* and *NvFz5/8* display a moderate, but consistent expansion towards the oral pole (Fig. 3G–I). For *NvWnt2* both the aboral and the oral boundaries of the belt-like expression domain are shifted towards the oral pole (Fig. 3J). As shown in the insets in Fig. 3J and K, in *NvGpc1/2/4/6* morphants the *NvWnt2* expression appears to overlap partially with that of *NvFkh* around the oral opening, which is free of *NvWnt2* expression in control animals (insets in Fig. 3D and E). The expression of *NvFkh* is only slightly impaired, with a small shift of the aboral boundary of the expression domain towards the oral pole (Fig. 3K). Using *NvSulf* as an

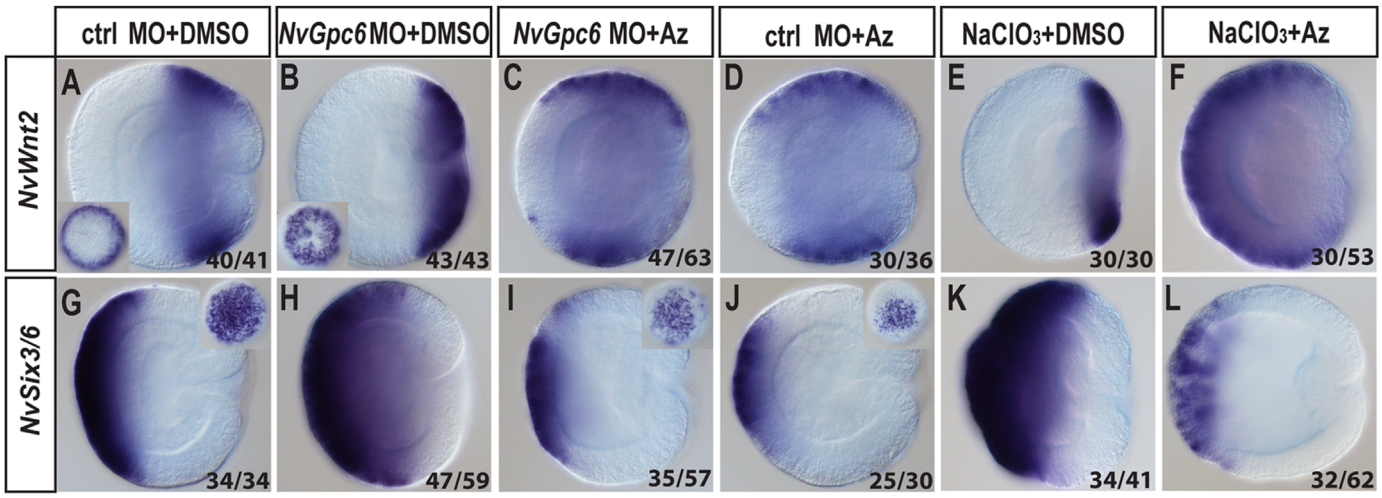

Fig. 4. ***NvGpc1/2/4/6*** **MO and** $NaClO_3$ **treatment phenotypes can be overcome by β-catenin overactivation**. **(A–L)** Lateral views of in situ hybridisations at mid-gastrula stage with aboral pole to the left; insets in top right corners (in **G, I** and **J**) are aboral views, insets in bottom left corners (in **A** and **B**) are oral views. *NvGpc1/2/4/6* MO injected and $NaClO_3$ treated animals treated with 1 μM azakenpaullone (Az) from early-blastula stage on show the same pattern changes as mismatch MO injected animals treated with Az. Numbers indicate the proportion of animals showing the depicted phenotype.

additional marker gene revealed that its expression in the oral half of the ectoderm is shifted orally, whereas its uniform expression in the endoderm is unaffected (Fig. 3F and L).

We confirmed these changes in the spatial expression patterns by quantitative RT-PCR (RT-qPCR). All tested aboral markers (*NvFGFa1*, *NvFGFa2*, *NvFGFRa*, *NvSix3/6*, *NvFoxQ2a* and *NvFz5/8*) were upregulated and the oral half markers *NvWnt2* and *NvFkh* were downregulated at gastrula stage in *NvGpc1/2/4/6* morphants (Fig. 3W). The expansion of aboral and the reduction of oral markers in *NvGpc1/2/4/6* morphants at gastrula stage is highly similar to that observed in *NvFz5/8* morphants (Fig. 3V and Leclère et al., 2016), but it is not found in *NvFGFa1* or *NvFGFRa* morphants (Rentzsch et al., 2008; Sinigaglia et al., 2013). *NvFGFa2* expression is slightly reduced in *NvFGFa1* morphants (Fig. 3S), as reported previously (Sinigaglia et al., 2013), but *NvSix3/6* and *NvWnt2* are not affected at gastrula stage (Fig. 3T and U).

The 6-O sulfation status of heparan sulfate has been shown to affect Wnt and FGF signalling (Ai et al., 2003; Wang et al., 2004). Since the expression of *NvSulf* is restricted to the oral hemisphere at blastula and gastrula stages and the expression of *NvHS6OST* commences at blastula stage (Feta et al., 2009), it is likely that the HS chains in the aboral domain are 6-O sulfated. To test whether sulfation is required for correct patterning of the oral-aboral axis, we treated embryos with the sulfation inhibitor sodium chlorate ($NaClO_3$; Humphries and Silbert, 1988; Safaiyan et al., 1999), which binds to ATP-sulphurylase and thereby prevents the generation of the sulfate donor 3′phosphoadenyl 5′phosphosulphate (PAPS; Farley et al., 1976). Concentrations between 10 and 50 mM gave similar results, whereas higher concentrations lead to increased mortality (data not shown). Treatment with 20 mM sodium chlorate lead to an expansion of the expression domains of *NvFGFa2*, *NvSix3/6* and *NvFz5/8* towards the oral pole; and to an oral shift of the *NvWnt2* expression domain (Fig. 3M–P), strikingly similar to knockdown of *NvGpc1/2/4/6* (Fig. 3G–J). However, unlike *NvGpc1/2/4/6* knockdown, the expression of *NvFkh* and *NvSulf* were hardly affected (Fig. 3Q and R). All expression changes were confirmed by RT-qPCR analysis (Fig. 3(W)). While the expression of the broad aboral domain markers *NvSix3/6*, *NvFoxQ2a*, *NvFGFRa* and *NvFz5/8* was upregulated to a similar extent in $NaClO_3$ treated and in *NvGpc1/2/4/6* MO-injected animals, the upregulation of the more restricted aboral markers *NvFGFa1* and *NvFGFa2* was 4–6fold higher in $NaClO_3$ treated animals than in *NvGpc1/2/4/6* morphants (Fig. 3W). This difference is also reflected in the spatial expansion of the expression domain (Fig. 3A, G and M).

3.4. *NvGpc1/2/4/6 MO and* $NaClO_3$ *treatment phenotypes can be rescued by Nvβ-catenin overactivation*

The similarity of the changes in expression domains in *NvGpc1/2/4/6* morphants and $NaClO_3$ treated animals compared to *NvFz5/8* morphants prompted us to investigate whether they can be affected by manipulation of Wnt/β-catenin signalling. The patterning changes in *NvFz5/8* morphants can be rescued by pharmaceutical overactivation of canonical Wnt/β-catenin signalling (Leclère et al., 2016). In a similar experiment the shift of *NvWnt2* expression towards the oral pole and the expansion of *NvSix3/6* expression in *NvGpc1/2/4/6* morphants were suppressed by exposure of the injected animals to a low dose (1 μM) of azakenpaullone from early cleavage stages on (Fig. 4A–C and G–I). The double-treated animals instead resembled those injected with the control MO and treated with azakenpaullone (Fig. 4D and J). Similarly, treatment with azakenpaullone prevented the effects of $NaClO_3$ treatment (Fig. 4E, F, K and L). These experiments are consistent with a model in which NvGpc1/2/4/6 and HS sulfation act at the plasma membrane of cells that activate Nvβ-catenin in response to Wnt signalling during axial patterning.

3.5. *NvGpc1/2/4/6 morphants have a reduced apical tuft*

After gastrulation, *Nematostella* embryos elongate along the oral-aboral axis into a slightly pear-shaped planula that is wider at the oral pole than at the aboral pole. At mid-planula stage the apical organ with a prominent tuft of long cilia develops at the aboral pole (Hand and Uhlinger, 1992; Lee et al., 2007). Upon *NvGpc1/2/4/6* knockdown, both the elongation of the axis and the formation of the apical tuft were affected. The animals remained more rounded, the length and diameter of the apical tuft were reduced (Fig. 5A–F) and the animals did not develop into polyps. We classified the animals into three categories of increasing severity of the planula phenotype. In animals with the weakest phenotype, the aboral domain was wider than in WT planulae and the apical tuft was slightly reduced (“small tuft” phenotype in Figs. 6A and S3). The intermediate phenotype had a clearly reduced apical tuft and the aboral domain was wider than the oral domain (“aborally rounded” phenotype). In the most severe phenotype, the apical organ was almost invisible (only detectable by immunostaining of the cilia) and the animals were almost

completely round ("rounded" phenotype). Injection of different concentrations of the morpholino showed that the strength of the phenotype correlates with the amount of MO injected (Fig. 6A). Thus, despite the expansion of aboral marker gene expression at gastrula stage (Fig. 3l–M, W), the apical tuft is reduced in *NvGpc1/2/4/6* knockdown animals at planula stage.

3.6. At planula stage aboral patterning is disrupted upon NvGpc1/2/4/6 knockdown

To better understand the basis for the reduction in apical tuft size we analysed the expression of several marker genes for different regions within the aboral domain. At planula stage, *NvSix3/6* is expressed in a broad aboral domain, but it is excluded from a spot at the aboral pole, from which the apical organ develops (n=47; Fig. 7A). After injection of *NvGpc1/2/4/6* MO, 64% of the animals displayed the wildtype expression, however, 36% had no gap in the *NvSix3/6* expression at the aboral pole (n=53; Fig. 7B and C). *NvFGFa2* is expressed in the *NvSix3/6*-free spot at the aboral pole and this expression is also observed in the *NvGpc1/2/4/6* knockdown animals (Fig. 7D and E).

NvFoxJ1, which has a conserved role in controlling ciliogenesis in other animals (Sinigaglia et al., 2015; Thomas et al., 2010), shows an even less homogeneous response to *NvGpc1/2/4/6* knockdown (n=69; Fig. 8O): 35% of the injected animals showed close to WT expression (Fig. 7F and data not shown), in 29% the spot-like expression domain was strongly reduced (Fig. 7G), 25% showed no expression, whereas 11% showed an expanded domain (Fig. 7H). Consistent with the reduced staining in most animals, RT-qPCR analysis confirmed a slight downregulation of *NvFoxJ1* in *NvGpc1/2/4/6* morphants at planula stage (Fig. 9).

NvTauD (Taurine catabolism dioxygenase) and *NvMeprin-like* (a

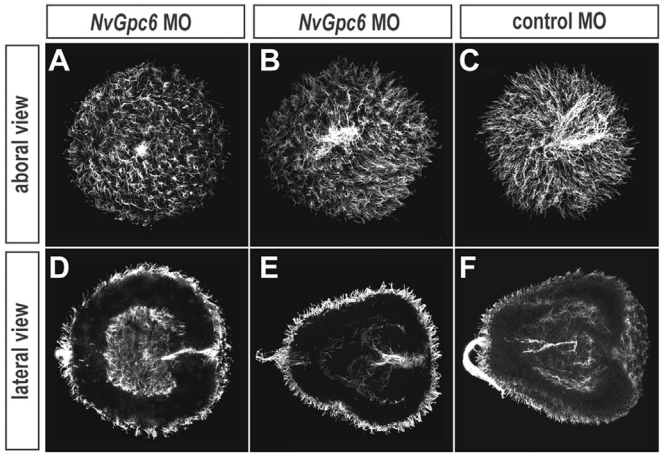

Fig. 5. *NvGpc1/2/4/6* morphants have a reduced apical organ and an altered body shape. (A–F) Cilia are stained with anti-acetylated tubulin antibody (white) at planula stage, **(A–C)** aboral views, **(D–F)** lateral views with aboral to the left. *NvGpc1/2/4/6* morphants (**A** and **B, D** and **E**) have reduced apical tufts, both in diameter and length, compared to control MO injected animals (**C** and **F**). Phenotypes of varying severity can be distinguished in *NvGpc1/2/4/6* morphants, (**A** and **D**) is more severe than (**B** and **E**), as seen by the reduced tuft and more rounded shape of (**A** and **D**). For phenotypic abundances see Fig. 6A. **(A-F)** Maximum projections of confocal stacks.

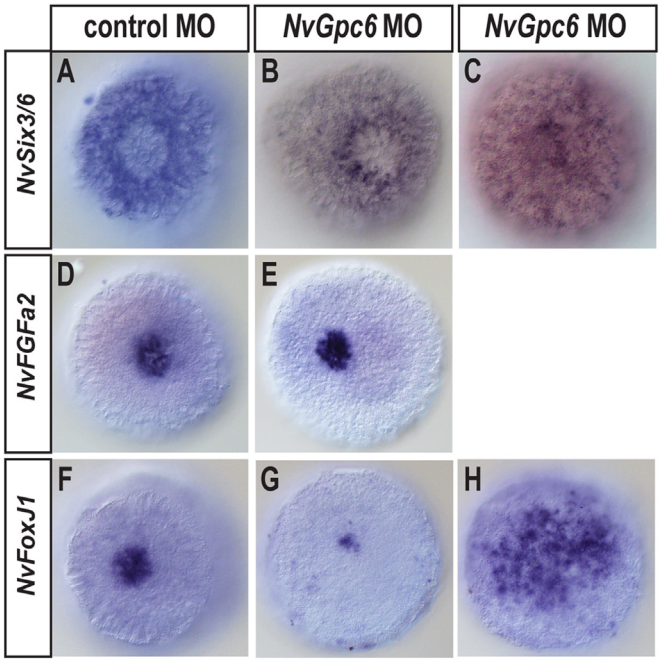

Fig. 7. Patterning of the aboral pole and the apical organ is fine-tuned by *NvGpc1/2/4/6*. (A–H) Aboral views of in situ hybridisations of planulae. Expression changes of different genes in *NvGpc1/2/4/6* morphants showed different degrees of severity. **(A–C)** In morphants, *NvSix3/6* was either expressed in a similar ring as in WT animals **(B)**, or in a pattern where the gap in the ring was lost **(C). (D and E)** *NvFGFa2* showed no change in expression in morphants. **(F–I)** *NvFoxJ1* expression was either slightly reduced (not shown), or reduced to a tiny spot **(G)**. 11% of *NvGpc1/2/4/6* knockdown animals exhibit an expanded *NvFoxJ1* expression domain **(H)**. For abundance of phenotypes/gene see graph in Fig. 8O.

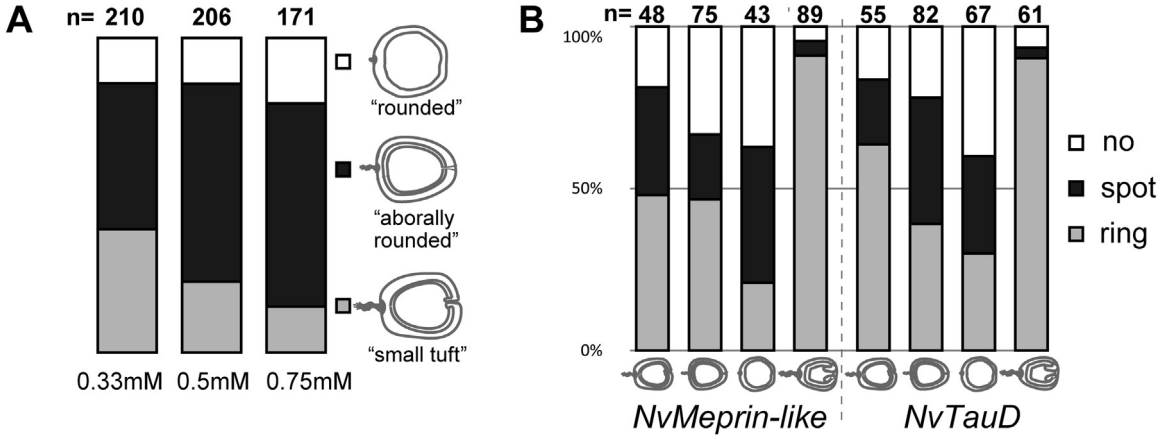

Fig. 6. The morphological severity of *NvGpc1/2/4/6* knockdown phenotypes correlates with patterning changes at the aboral pole. (A) Severity of *NvGpc1/2/4/6* morpholino knockdown phenotypes is dose dependent. **(B)** Expression patterns for *NvMeprin-like* and *NvTauD* were scored, and the relative abundance of each pattern is plotted for each morphological phenotype (see Fig. S3 for phenotype sketches) and for control morpholino injected animals; "no" refers to undetectable expression.

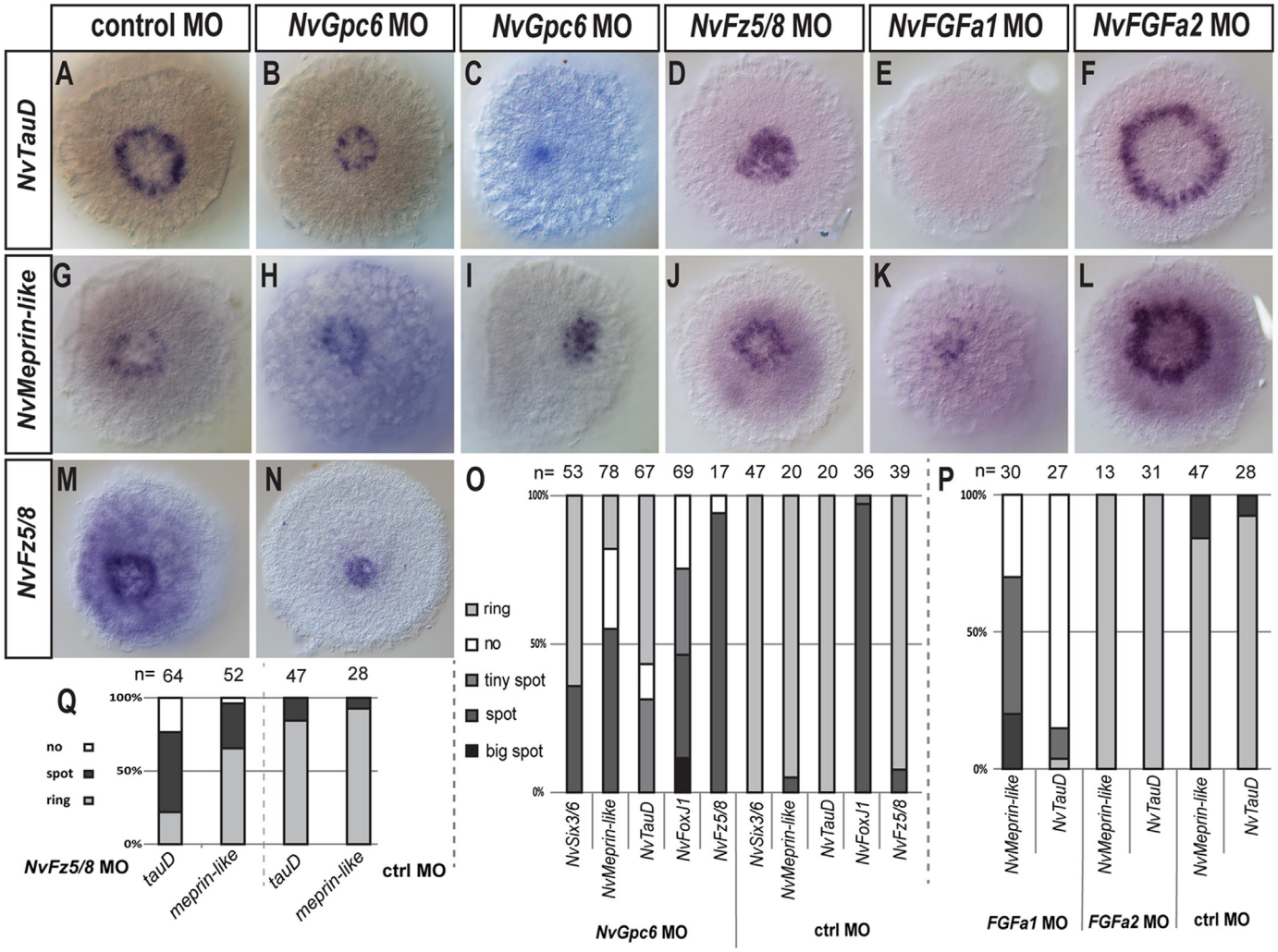

Fig. 8. Patterning changes within the apical organ upon *NvGpc1/2/4/6* knockdown display similarities to *NvFz5/8* and *NvFGFa1* knockdown. (A–N) ISHs of planulae, all panels are aboral views. For *NvGpc1/2/4/6* knockdown two phenotypes are shown for *NvMeprin-like* and *NvTauD* expression: **(B and H)** show ring expression reduced in diameter; **(C and I)** expression domain collapsed to a (tiny in **C**) spot; **(N)** *NvFz5/8* expression domain was reduced to a spot in 94% of the animals (absent expression not shown). **(D and J)** *NvFz5/8* knockdown exhibits similar effects to a weak *NvGpc1/2/4/6* MO phenotype. **(E and K)** *NvFGFa1* knockdown leads to loss or massive reduction of expression. **(F and L)** *NvFGFa2* knockdown expands the diameter of the ring domain substantially. **(O–Q)** Quantification of expression phenotypes in the indicated knockdown experiments, "no" indicates undetected expression. See also Fig. S5.

MAM domain containing metalloprotease) were identified based on their regulation by FGF signalling; they are expressed in small ring-like subsets of the apical organ cells at the aboral pole at planula stage (Fig. 8A and G). In contrast to *NvTauD*, *NvMeprin-like* is already expressed at gastrula stage, in a contiguous domain at the aboral pole (Sinigaglia et al., 2015). *NvFz5/8* is broadly expressed in the aboral domain, with stronger expression in a ring domain at the aboral pole (Fig. 8M; Leclère et al., 2016). It is not clear whether these three genes are partially or entirely co-expressed and how their expression domain precisely relates to the apical organ forming domain.

For *NvTauD* (n=67) and *NvMeprin-like* (n=78) three phenotypes were observed in *NvGpc1/2/4/6* knockdown animals: a ring-like domain with a smaller diameter (Fig. 8B, H and O) occurred in 15% for *NvMeprin-like* and in 57% for *NvTauD*, a small spot-like expression (Fig. 8C, I and O) was observed in 31% for *NvTauD* and 55% for *NvMeprin-like*, or a loss of expression. Sorting of the *NvGpc1/2/4/6* knockdown animals into the above described morphological categories ("small tuft", "aborally rounded" and "rounded") prior to in situ hybridisation showed that the percentage of animals in which the WT ring expression pattern transformed into a spot-like expression, or loss of expression, increased with the severity of the morphological phenotype (Fig. 6A and B).

To better understand the effects of *NvGpc1/2/4/6* knockdown on the expression of *NvTauD* and *NvMeprin-like*, we analysed their expression patterns after knockdown of other genes that are involved in the patterning of the aboral domain and the development of the apical organ. In *NvFGFa1* morphants, the expression of *NvTauD* and *NvMeprin-like* was reduced or absent in >80% of the animals (Fig. 8E, K and P), whereas their ring of expression became much wider in *NvFGFa2* morphants (Fig. 8F, L and P), consistent with the previously described roles of these two FGFs as positive and negative regulators of apical organ development, respectively (Rentzsch et al., 2008; Sinigaglia et al., 2015). In *NvFz5/8* morphants, which in most cases develop an apical tuft (Leclère et al., 2016), the expression of *NvTauD* and *NvMeprin-like* either remained in a ring or became a spot, in contrast to *NvGpc1/2/4/6* morphants, the diameter of the ring or spot was not reduced compared to controls (Fig. 8D, J and Q).

When comparing the penetrance of the changes in expression patterns, we noticed that in *NvFz5/8* morphants the expression of *NvTauD* was more frequently affected than that of *NvMeprin-like* (78% of the animals for *NvTauD* vs. 35% for *NvMeprin-like*). Similarly, in *NvFGFa1* morphants, *NvTauD* expression was more strongly affected

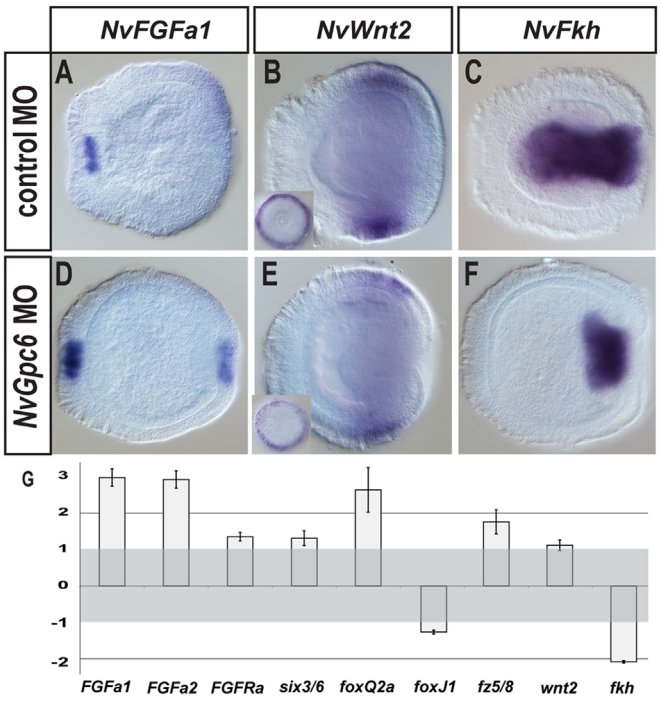

Fig. 9. Effects of *NvGpc1/2/4/6* knockdown on axial patterning genes at planula stage. (A–F) In situ hybridisations of planulae, lateral views, oral is to the right. *NvGpc1/2/4/6* knockdown leads to upregulation of *NvFGFa1* **(G)** and ectopic oral expression **(D)**. *NvWnt2* expression is not affected at planula stage (cf. gastrula stage), neither in abundance **(G)** nor pattern **(E)**. *NvFkh* expression is down-regulated and the domain strongly reduced (this is likely due to the observed malformation/underdevelopment of the pharynx) (**F** and **G**). **(G)** Analysis of axial patterning genes by RT-qPCR (see Section 2 for details).

(85% no expression) than that of *NvMeprin-like* (30% no expression; 50% a tiny spot) (Fig. 8P). In contrast, in *NvGpc1/2/4/6* morphants, the ring-like expression was lost in 82% of the animals for *NvMeprin-like*, but in only 43% for *NvTauD* (Fig. 8O), revealing a more consistent effect on *NvMeprin-like*. The expression of *NvFz5/8* itself was reduced to a small spot in 94% of the *NvGpc1/2/4/6* morpholino injected animals (Fig. 8M–O), whereas *NvFGFa1* and *NvFGFa2* do not seem to be affected upon *NvGpc1/2/4/6* knockdown (Fig. 7D and E and Fig. 9A and D). At gastrula stage, the contiguous expression domain of *NvMeprin-like* is expanded by knockdown of *NvGpc1/2/4/6*, similar to all other aboral markers (Fig. S4).

3.7. *Patterning within the aboral pole of the planula is affected by sodium chlorate treatment*

Having found that *NvGpc1/2/4/6* plays a role in both early patterning along the oral-aboral axis and in patterning within the aboral pole at planula stage, and that *NvGpc1/2/4/6*'s early role is likely dependent on the sulfation of HS chains, we wanted to know if this particular modification of HS chains also plays a role in the later function of *NvGpc1/2/4/6*.

We treated animals for different periods of time with sodium chlorate (Fig. 10K) and fixed them at mid-planula stage (72 hpf at 21 °C) Treated animals showed four different patterning effects: *NvMeprin-like* was either expressed in a much expanded spot (Fig. 10A), a spot matching the size of the WT ring domain (Fig. 10B), a broader and thicker ring (Fig. 10C) or a ring which was roughly of wildtype size (Fig. 10D). The different treatment periods caused these four phenotypes in different proportions as quantified in Fig. 10L, revealing that continuous treatment from early development has the most profound effects. In the majority of animals treated from 6.5 to 72 hpf (67%) or from 24 to 72 hpf (92%), the expression of *NvMeprin-like* was expanded, either as a ring or as a wider spot. Interestingly, while both treatment schemes led to an expanded region of *NvMeprin-like* expression, only the treatment from 6.5 to 72 hpf led to high percentage of animals with an expanded spot (50% in 6.5–72 hpf, 5% in 24–72 hpf treatment), whereas most animals after 24–72 hpf treatment expressed *NvMeprin-like* in a wide ring (88% vs. 19%). In contrast, treatment from 48 to 72 hpf resulted mainly in expression in WT-sized rings (75%). This suggests that until mid-gastrulation (24 hpf) sulfation of GAGs is important to initiate the suppression of *NvMeprin-like* expression in the aboral-most territory, thus leading to the later ring-like expression.

The expression of *NvTauD* was also more severely affected by treatment which initiated in early development. The main effect, however, was a loss of expression (> 40% of animals), which was never observed for *NvMeprin-like*. Treatment from 24 or 48 hpf had only a mild effect on *NvTauD* expression. Taken together, the sodium chlorate treatments suggest that GAG sulfation has an important role mainly during early development and the different effects on *NvMeprin-like* and *NvTauD* indicate that these two genes are either not expressed in precisely the same cells, or that their expression is differentially controlled by Wnt and/or FGF signalling.

4. Discussion

Glypicans are indispensable regulators of several signalling pathways during embryonic development in bilaterians. In this study we identify a developmental function for a glypican in the sister group to the Bilateria, the Cnidaria. Knockdown of *NvGpc1/2/4/6* results in gene expression changes that are highly similar to those observed in *NvFz5/8* knockdown animals and both knockdowns can be rescued by overactivation of Nvβ-catenin, suggesting that one function of *NvGpc1/2/4/6* is the positive regulation of NvFz5/8-mediated Wnt signalling.

4.1. *Possible mechanisms for the regulation of NvFz5/8 by NvGpc1/2/4/6*

The evidence for the regulation of NvFz5/8 signalling by NvGpc1/2/4/6 is currently only indirect, i.e. based on the similarity of the phenotypes upon knockdown. Nevertheless, in line with more detailed studies in *Drosophila* and in vertebrates, two mechanisms for the potential regulation of NvFz5/8 signalling by NvGpc1/2/4/6 are conceivable. NvGpc1/2/4/6 might serve as a co-receptor that facilitates the interaction between a Wnt ligand and the NvFz5/8 receptor. Such a mechanism has been suggested to explain the function of Dally (the *Drosophila glypican 3/5* ortholog) in Wnt/Wg signalling in the wing imaginal disc (Franch-Marro et al., 2005; Han et al., 2005; Yan et al., 2009). A co-receptor function would most likely be based on the binding of glypicans to Wnts (Ai et al., 2003; Ohkawara et al., 2003; Song et al., 2005), but might also utilise binding to Frizzled (Capurro et al., 2014; Ohkawara et al., 2003) to augment the activation of the pathway.

In a second scenario, NvGpc1/2/4/6 could facilitate the movement of a Wnt ligand towards the *NvFz5/8* expressing domain. Increased movement of Wnt ligands has been suggested as the mechanism by which dlp (the *Drosophila glypican1/2/4/6* ortholog) promotes Wnt signalling activity distant to the source of the Wnt ligand (Franch-Marro et al., 2005) and HSPGs have been shown to increase the solubility of vertebrate Wnts (Fuerer et al., 2010). In *Nematostella*, the expression of *Wnt* ligands is restricted to the oral hemisphere of the embryo (Kusserow et al., 2005). The most aborally expressed ectodermal Wnt (*NvWnt2*) abuts or slightly overlaps with the aboral expression domain of *NvFz5/8*. The expression of *NvGpc1/2/4/6*, however, encompasses most of the oral-

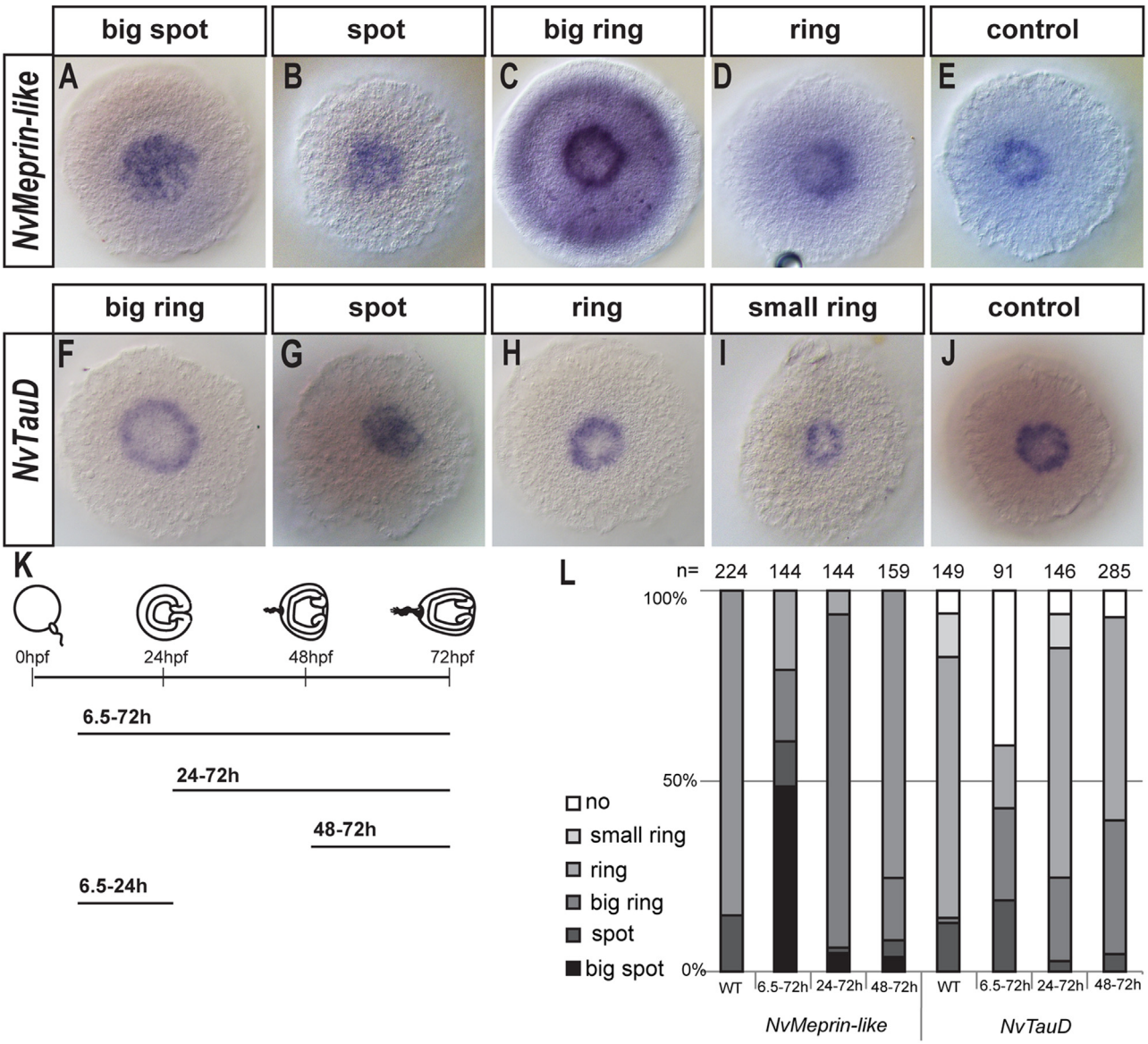

Fig. 10. Sodium chlorate treatment reveals that HS sulfation regulates aboral patterning throughout larval development. (A–J) In situ hybridisations, all panels show aboral views of planula larvae. Two types of patterning change can be observed, the first is expansion (**A, C** and **F**) or reduction **(I)** of the diameter of the expression domain and the second is ectopic expression in the centre of the ring domain (**A, B** and **G**). **(K)** Scheme of drug treatment periods. **(L)** Quantification of expression phenotypes in each condition. *NvMeprin-like* expression is more strongly affected than *NvTauD* expression, with early treatment causing the most severe defects in gene patterning.

aboral axis, overlapping with *NvFz5/8* and *NvWnt2*, and might thus enhance movement of Wnt ligands from sending to receiving cells. In this context we find it interesting to note that Dlp has been shown to promote Wnt signalling activity at low levels of Wnt ligand, but to reduce Wnt activity at high levels of ligands (Kreuger et al., 2004; Yan et al., 2009). Such a biphasic activity might help to explain why *NvGpc1/2/4/6* appears to be required rather for low level Wnt signalling in the aboral domain than for high level signalling in the more oral *NvWnt2* expressing domain. At a more general level, a role of *NvGpc1/2/4/6* that affects the distribution and signalling range of Wnt ligands would defy any strict classification as an agonist or antagonist (Lander, 2007). Clearly, data about physical interactions of NvGpc1/2/4/6 and Wnt signalling components and their potential effect on Wnt signalling will be essential to obtain a better understanding of the role of NvGpc1/2/4/6 in *Nematostella* development.

4.2. Sulfation of proteoglycans is an evolutionary conserved mechanism to regulate extracellular signalling

Sulfation of heparan sulfate has been shown to regulate Wnt signalling either positively (Lin and Perrimon, 1999; Reichsman et al., 1996) or negatively (Ai et al., 2003; Dhoot et al., 2001; Kleinschmit et al., 2013); at least partially depending on the particular Wnt ligand (Fellgett et al., 2015). Similarly, Sulf1 has a positive role in Wnt signalling in vertebrates (Ai et al., 2003; Dhoot et al., 2001; Nawroth et al., 2007), but it acts as a negative regulator of Wnt activity in *Drosophila* (Kleinschmit et al., 2013; You et al., 2011).

The similarity of the patterning defects of sodium chlorate treatment, *NvFz5/8* and *NvGpc1/2/4/6* knockdown suggests that during early development of *Nematostella*, sulfation of NvGpc1/2/4/6 might positively regulate low level Wnt signalling in the aboral domain. The sodium chlorate concentration that we have used

preferentially disrupts 6-O sulfation in cell culture (Safaiyan et al., 1999) and the expression of the HS 6-O desulfating enzyme *NvSulf* is restricted to the oral hemisphere of the ectoderm at gastrula stage. These observations make it tempting to speculate that HS 6-O sulfation is the key HS modification for the regulation of aboral Wnt signalling. This means that both scenarios described above might be true; oral desulfation in the 6-O position would enhance Wnt diffusion, whereas aborally the 6-O-sulfated HS chains would facilitate NvGpc1/2/4/6 co-receptor activity.

However, sodium chlorate can also desulfate chondroitin sulfate chains (Greve et al., 1988; Humphries and Silbert, 1988) and its specificity at different concentrations might differ between organisms. We also note that we cannot rule out that NvGpc1/2/4/6 and GAG sulfation affect currently uncharacterised functions of Hedgehog or TGFβ signalling and that such a function could secondarily affect Wnt signalling. Neither Hedgehog nor TGFβ signalling have been shown to play a role in oral-aboral patterning in *Nematostella*, though.

4.3. Roles of NvGpc1/2/4/6 and sulfation at planula stage

After gastrulation, the aboral territory becomes patterned into smaller domains and the regulatory interactions among aboral patterning genes change significantly (Leclère et al., 2016; Sinigaglia et al., 2013). Coincident with these changes, the effects of *NvGpc1/2/4/6* knockdown were more variable at planula than at gastrula stage, for example, the aboral and oral markers no longer showed a uniform response (Figs. 7–9). Still, it is currently not possible to conclude whether the observed changes in morphology and expression of marker genes in planulae derive from the early patterning role of *NvGpc1/2/4/6* or from a distinct function after gastrulation.

The expression of *NvFGFa1*, *NvSix3/6*, *NvTauD* and *NvMeprin-like* after *NvGpc1/2/4/6* knockdown shows similarity to *NvFz5/8* knockdown animals, but is clearly different from *NvFGFa1* knockdown (Leclère et al., 2016; Sinigaglia et al., 2013). However, at planula stage *NvFz5/8* morphants display a dramatic compression of the oral-aboral axis that develops after gastrulation and that we do not observe in *NvGpc1/2/4/6* morphants, and this suggests that functions of NvFz5/8 after gastrulation are not regulated by NvGpc1/2/4/6.

The sodium chlorate treatments showed that GAG sulfation is particularly important at blastula and gastrula stages, corresponding with the upregulation of *NvHS6OST* (HS 6-O-sulfotransferase), *NvHS3OST* and *NvSulf* at this stage (Feta et al., 2009). This supports a model in which sulfation of HS chains on NvGpc1/2/4/6 is particularly important for NvFz5/8 signalling during early development although treatments at later stages still resulted in some patterning defects. In contrast to *NvTauD*, *NvMeprin-like* is in WT animals already expressed at gastrula stage in a broad aboral domain which becomes restricted and ring-like after gastrulation (Sinigaglia et al., 2015). Sodium chlorate treatment from both early blastula and gastrula stage on (6.5–72 hpf and 24–72 hpf, respectively) resulted in a broadened expression domain, but only treatment from early blastula stage on prevented the development of the ring-like expression domain with a gap at the aboral pole in a significant proportion of embryos (48% vs. 4%). This indicates two at least temporally distinct functions for sulfated GAGs in the fine tuning of the patterning of the aboral domain: first in the specification of the aboral-most territory (which is free of *NvMeprin-like* expression after gastrulation), and subsequently in the restriction of a broader aboral area. Addressing how these distinct functions relate to *NvGpc1/2/4/6* and the regulation of signalling pathways will require the development of methods to temporally control gene function in *Nematostella*.

4.4. Glypicans and axial patterning

Expression data and functional studies on the role of glypicans in early development are limited to few species. In zebrafish and *Xenopus*, glypican 4 regulates non-canonical Wnt signalling and in consequence the elongation of the anterior-posterior body axis by convergent-extension tissue movements (Galli et al., 2003; Ohkawara et al., 2003; Topczewski et al., 2001). In sea urchin, *glypican 5* is expressed on the dorsal side and may regulate signalling by the TGFβ ligands nodal and/or Bmp2/4 in conjunction with sulfated GAGs (Bergeron et al., 2011; Lapraz et al., 2009). A role in the patterning of the primary body axis has to our knowledge not been described; studies on a broader range of taxa will be required to determine whether this function is evolutionarily conserved or a novelty of *Nematostella* development.

5. Conclusions

We show here that the patterning of the oral-aboral axis in *Nematostella* embryos is dependent on spatial and temporal expression dynamics of glypicans and on heparan sulfate chains. NvGlypican1/2/4/6 likely acts as a co-factor that promotes signalling by NvFrizzled5/8, suggesting that the modulation of Wnt signalling is an ancient function of glypicans that evolved prior to the divergence of cnidarians and bilaterians. However, the effects of *NvGpc1/2/4/6* knockdown at planula stage indicate that NvGlypican1/2/4/6 may also regulate additional signalling pathways that contribute to the fine patterning of the aboral domain and the apical organ.

Acknowledgements

We thank Gemma Richards for help with the morpholino control experiments and for critical reading of the manuscript, Maja Adamska and Marcin Adamski for sharing *Sycon ciliatum* transcriptome data before publication, Bård Steinar Giezendanner and Justine Emmanuelle Diaz for maintaining the *Nematostella* culture and the members of the Rentzsch lab for discussions. Research in FR's lab is funded by the Sars Centre core budget.

Appendix A. Supporting information

Supplementary data associated with this article can be found in the online version at http://dx.doi.org/10.1016/j.ydbio.2016.04.011.

References

Ai, X., Do, A.T., Lozynska, O., Kusche-Gullberg, M., Lindahl, U., Emerson Jr., C.P., 2003. QSulf1 remodels the 6-O sulfation states of cell surface heparan sulfate proteoglycans to promote Wnt signaling. J. Cell Biol. 162, 341–351.
Akam, M., Averof, M., Castelli-Gair, J., Dawes, R., Falciani, F., Ferrier, D., 1994. The evolving role of Hox genes in arthropods. Dev. Suppl., 209–215.
Bergeron, K.F., Xu, X., Brandhorst, B.P., 2011. Oral-aboral patterning and gastrulation of sea urchin embryos depend on sulfated glycosaminoglycans. Mech. Dev. 128, 71–89.
Bernfield, M., Gotte, M., Park, P.W., Reizes, O., Fitzgerald, M.L., Lincecum, J., Zako, M., 1999. Functions of cell surface heparan sulfate proteoglycans. Annu. Rev. Biochem. 68, 729–777.
Bishop, J.R., Schuksz, M., Esko, J.D., 2007. Heparan sulphate proteoglycans fine-tune mammalian physiology. Nature 446, 1030–1037.
Bulow, H.E., Hobert, O., 2006. The molecular diversity of glycosaminoglycans shapes animal development. Annu. Rev. Cell Dev. Biol. 22, 375–407.
Capurro, M., Martin, T., Shi, W., Filmus, J., 2014. Glypican-3 binds to Frizzled and plays a direct role in the stimulation of canonical Wnt signaling. J. Cell Sci. 127, 1565–1575.
Dhoot, G.K., Gustafsson, M.K., Ai, X., Sun, W., Standiford, D.M., Emerson Jr., C.P.,

2001. Regulation of Wnt signaling and embryo patterning by an extracellular sulfatase. Science 293, 1663–1666.
Esko, J.D., Kimata, K., Lindahl, U., 2009. Proteoglycans and sulfated glycosaminoglycans. In: Varki, A., Cummings, R.D., Esko, J.D., Freeze, H.H., Stanley, P., Bertozzi, C.R., Hart, G.W., Etzler, M.E. (Eds.), Essentials of Glycobiology, 2nd ed Cold Spring Harbor, NY.
Esko, J.D., Selleck, S.B., 2002. Order out of chaos: assembly of ligand binding sites in heparan sulfate. Annu. Rev. Biochem. 71, 435–471.
Esko, J.D., Zhang, L., 1996. Influence of core protein sequence on glycosaminoglycan assembly. Curr. Opin. Struct. Biol. 6, 663–670.
Farley, J.R., Cryns, D.F., Yang, Y.H., Segel, I.H., 1976. Adenosine triphosphate sulfurylase from penicillium chrysogenum. Steady state kinetics of the forward and reverse reactions. J. Biol. Chem. 251, 4389–4397.
Fellgett, S.W., Maguire, R.J., Pownall, M.E., 2015. Sulf1 has ligand-dependent effects on canonical and non-canonical Wnt signalling. J. Cell Sci. 128, 1408–1421.
Feta, A., Do, A.T., Rentzsch, F., Technau, U., Kusche-Gullberg, M., 2009. Molecular analysis of heparan sulfate biosynthetic enzyme machinery and characterization of heparan sulfate structure in *Nematostella vectensis*. Biochem. J. 419, 585–593.
Fico, A., Maina, F., Dono, R., 2011. Fine-tuning of cell signaling by glypicans. Cell. Mol. Life Sci. 68, 923–929.
Filmus, J., Capurro, M., Rast, J., 2008. Glypicans. Genome Biol. 9, 224.
Finnerty, J.R., Pang, K., Burton, P., Paulson, D., Martindale, M.Q., 2004. Origins of bilateral symmetry: Hox and dpp expression in a sea anemone. Science 304, 1335–1337.
Franch-Marro, X., Marchand, O., Piddini, E., Ricardo, S., Alexandre, C., Vincent, J.P., 2005. Glypicans shunt the Wingless signal between local signalling and further transport. Development 132, 659–666.
Fritzenwanker, J.H., Genikhovich, G., Kraus, Y., Technau, U., 2007. Early development and axis specification in the sea anemone *Nematostella vectensis*. Dev. Biol. 310, 264–279.
Fritzenwanker, J.H., Saina, M., Technau, U., 2004. Analysis of forkhead and snail expression reveals epithelial-mesenchymal transitions during embryonic and larval development of *Nematostella vectensis*. Dev. Biol. 275, 389–402.
Fritzenwanker, J.H., Technau, U., 2002. Induction of gametogenesis in the basal cnidarian *Nematostella vectensis* (Anthozoa). Dev. Genes Evol. 212, 99–103.
Fuerer, C., Habib, S.J., Nusse, R., 2010. A study on the interactions between heparan sulfate proteoglycans and Wnt proteins. Dev. Dyn. 239, 184–190.
Galli, A., Roure, A., Zeller, R., Dono, R., 2003. Glypican 4 modulates FGF signalling and regulates dorsoventral forebrain patterning in Xenopus embryos. Development 130, 4919–4929.
Gellon, G., McGinnis, W., 1998. Shaping animal body plans in development and evolution by modulation of Hox expression patterns. BioEssays 20, 116–125.
Greve, H., Cully, Z., Blumberg, P., Kresse, H., 1988. Influence of chlorate on proteoglycan biosynthesis by cultured human fibroblasts. J. Biol. Chem. 263, 12886–12892.
Hacker, U., Nybakken, K., Perrimon, N., 2005. Heparan sulphate proteoglycans: the sweet side of development. Nat. Rev. Mol. Cell Biol. 6, 530–541.
Hall, B.G., 2013. Building phylogenetic trees from molecular data with MEGA. Mol. Biol. Evol. 30, 1229–1235.
Han, C., Yan, D., Belenkaya, T.Y., Lin, X., 2005. Drosophila glypicans Dally and Dally-like shape the extracellular Wingless morphogen gradient in the wing disc. Development 132, 667–679.
Hand, C., Uhlinger, K., 1992. The culture, sexual and asexual reproduction, and growth of the sea anemone *Nematostella vectensis*. Biol. Bull. 182, 169–176.
Hejnol, A., Obst, M., Stamatakis, A., Ott, M., Rouse, G.W., Edgecombe, G.D., Martinez, P., Baguna, J., Bailly, X., Jondelius, U., Wiens, M., Muller, W.E.G., Seaver, E., Wheeler, W.C., Martindale, M.Q., Giribet, G., Dunn, C.W., 2009. Assessing the root of bilaterian animals with scalable phylogenomic methods. Proc. R. Soc. B 276, 4261–4270.
Humphries, D.E., Silbert, J.E., 1988. Chlorate: a reversible inhibitor of proteoglycan sulfation. Biochem. Biophys. Res. Commun. 154, 365–371.
Kirkpatrick, C.A., Knox, S.M., Staatz, W.D., Fox, B., Lercher, D.M., Selleck, S.B., 2006. The function of a Drosophila glypican does not depend entirely on heparan sulfate modification. Dev. Biol. 300, 570–582.
Kleinschmit, A., Takemura, M., Dejima, K., Choi, P.Y., Nakato, H., 2013. Drosophila heparan sulfate 6-O-endosulfatase Sulf1 facilitates wingless (Wg) protein degradation. J. Biol. Chem. 288, 5081–5089.
Kraus, Y., Technau, U., 2006. Gastrulation in the sea anemone *Nematostella vectensis* occurs by invagination and immigration: an ultrastructural study. Dev. Genes Evol. 216, 119–132.
Kreuger, J., Perez, L., Giraldez, A.J., Cohen, S.M., 2004. Opposing activities of Dally-like glypican at high and low levels of Wingless morphogen activity. Dev. Cell 7, 503–512.
Krumlauf, R., 1994. Hox genes in vertebrate development. Cell 78, 191–201.
Kumburegama, S., Wijesena, N., Xu, R., Wikramanayake, A.H., 2011. Strabismus-mediated primary archenteron invagination is uncoupled from Wnt/beta-catenin-dependent endoderm cell fate specification in *Nematostella vectensis* (Anthozoa, Cnidaria): implications for the evolution of gastrulation. EvoDevo 2, 2.
Kusserow, A., Pang, K., Sturm, C., Hrouda, M., Lentfer, J., Schmidt, H.A., Technau, U., von Haeseler, A., Hobmayer, B., Martindale, M.Q., Holstein, T.W., 2005. Unexpected complexity of the Wnt gene family in a sea anemone. Nature 433, 156–160.
Lagutin, O.V., Zhu, C.C., Kobayashi, D., Topczewski, J., Shimamura, K., Puelles, L., Russell, H.R., McKinnon, P.J., Solnica-Krezel, L., Oliver, G., 2003. Six3 repression of Wnt signaling in the anterior neuroectoderm is essential for vertebrate forebrain development. Genes Dev. 17, 368–379.
Lander, A.D., 2007. Morpheus unbound: reimagining the morphogen gradient. Cell 128, 245–256.
Lapraz, F., Besnardeau, L., Lepage, T., 2009. Patterning of the dorsal-ventral axis in echinoderms: insights into the evolution of the BMP-chordin signaling network. PLoS Biol. 7, e1000248.
Layden, M.J., Rentzsch, F., Rottinger, E., 2016. The rise of the starlet sea anemone *Nematostella vectensis* as a model system to investigate development and regeneration. WIREs Dev. Biol. http://dx.doi.org/10.1002/wdev.1222
Leclère, L., Bause, M., Sinigaglia, C., Steger, J., Rentzsch, F., 2016. Development of the aboral domain in Nematostella requires β-catenin and the opposing activities of six3/6 and frizzled5/8. Development. http://dx.doi.org/10.1242/dev.120931.
Lee, P.N., Kumburegama, S., Marlow, H.Q., Martindale, M.Q., Wikramanayake, A.H., 2007. Asymmetric developmental potential along the animal-vegetal axis in the anthozoan cnidarian, *Nematostella vectensis*, is mediated by dishevelled. Dev. Biol. 310, 169–186.
Lin, X., 2004. Functions of heparan sulfate proteoglycans in cell signaling during development. Development 131, 6009–6021.
Lin, X., Perrimon, N., 1999. Dally cooperates with Drosophila Frizzled 2 to transduce Wingless signalling. Nature 400, 281–284.
Magie, C.R., Daly, M., Martindale, M.Q., 2007. Gastrulation in the cnidarian Nematostella vectensis occurs via invagination not ingression. Dev. Biol. 305, 483–497.
Mallo, M., Wellik, D.M., Deschamps, J., 2010. Hox genes and regional patterning of the vertebrate body plan. Dev. Biol. 344, 7–15.
Manuel, M., 2009. Early evolution of symmetry and polarity in metazoan body plans. C. R. Biol. 332, 184–209.
Marlow, H., Matus, D.Q., Martindale, M.Q., 2013. Ectopic activation of the canonical wnt signaling pathway affects ectodermal patterning along the primary axis during larval development in the anthozoan *Nematostella vectensis*. Dev. Biol. 380, 324–334.
Marlow, H., Tosches, M.A., Tomer, R., Steinmetz, P.R., Lauri, A., Larsson, T., Arendt, D., 2014. Larval body patterning and apical organs are conserved in animal evolution. BMC Biol. 12, 7.
Martin, B.L., Kimelman, D., 2009. Wnt signaling and the evolution of embryonic posterior development. Curr. Biol. 19, R215–R219.
Martindale, M.Q., Pang, K., Finnerty, J.R., 2004. Investigating the origins of triploblasty: 'mesodermal' gene expression in a diploblastic animal, the sea anemone *Nematostella vectensis* (phylum, Cnidaria; class, Anthozoa). Development 131, 2463–2474.
Matsuo, I., Kimura-Yoshida, C., 2013. Extracellular modulation of fibroblast growth factor signaling through heparan sulfate proteoglycans in mammalian development. Curr. Opin. Genet. Dev. 23, 399–407.
Matsuo, I., Kimura-Yoshida, C., 2014. Extracellular distribution of diffusible growth factors controlled by heparan sulfate proteoglycans during mammalian embryogenesis. Philos. Trans. R. Soc. Lond. Ser. B Biol. Sci., 369. http://dx.doi.org/10.1098/rstb.2013.0545.
Matus, D.Q., Magie, C.R., Pang, K., Martindale, M.Q., Thomsen, G.H., 2008. The Hedgehog gene family of the cnidarian, *Nematostella vectensis*, and implications for understanding metazoan Hedgehog pathway evolution. Dev. Biol. 313, 501–518.
Matus, D.Q., Thomsen, G.H., Martindale, M.Q., 2007. FGF signaling in gastrulation and neural development in *Nematostella vectensis*, an anthozoan cnidarian. Dev. Genes Evol. 217, 137–148.
Nakanishi, N., Renfer, E., Technau, U., Rentzsch, F., 2012. Nervous systems of the sea anemone *Nematostella vectensis* are generated by ectoderm and endoderm and shaped by distinct mechanisms. Development 139, 347–357.
Nawroth, R., van Zante, A., Cervantes, S., McManus, M., Hebrok, M., Rosen, S.D., 2007. Extracellular sulfatases, elements of the Wnt signaling pathway, positively regulate growth and tumorigenicity of human pancreatic cancer cells. PLoS One 2, e392.
Niehrs, C., 2010. On growth and form: a Cartesian coordinate system of Wnt and BMP signaling specifies bilaterian body axes. Development 137, 845–857.
Ohkawara, B., Yamamoto, T.S., Tada, M., Ueno, N., 2003. Role of glypican 4 in the regulation of convergent extension movements during gastrulation in *Xenopus laevis*. Development 130, 2129–2138.
Petersen, C.P., Reddien, P.W., 2009. Wnt signaling and the polarity of the primary body axis. Cell 139, 1056–1068.
Philippe, H., Brinkmann, H., Lavrov, D.V., Littlewood, D.T., Manuel, M., Worheide, G., Baurain, D., 2011. Resolving difficult phylogenetic questions: why more sequences are not enough. PLoS Biol. 9, e1000602.
Philippe, H., Derelle, R., Lopez, P., Pick, K., Borchiellini, C., Boury-Esnault, N., Vacelet, J., Renard, E., Houliston, E., Queinnec, E., Da Silva, C., Wincker, P., Le Guyader, H., Leys, S., Jackson, D.J., Schreiber, F., Erpenbeck, D., Morgenstern, B., Worheide, G., Manuel, M., 2009. Phylogenomics revives traditional views on deep animal relationships. Curr. Biol. 19, 706–712.
Posnien, N., Koniszewski, N.D., Hein, H.J., Bucher, G., 2011. Candidate gene screen in the red flour beetle Tribolium reveals six3 as ancient regulator of anterior median head and central complex development. PLoS Genet. 7, e1002416.
Reichsman, F., Smith, L., Cumberledge, S., 1996. Glycosaminoglycans can modulate extracellular localization of the wingless protein and promote signal transduction. J. Cell Biol. 135, 819–827.
Rentzsch, F., Fritzenwanker, J.H., Scholz, C.B., Technau, U., 2008. FGF signalling controls formation of the apical sensory organ in the cnidarian *Nematostella vectensis*. Development 135, 1761–1769.
Richards, G.S., Rentzsch, F., 2014. Transgenic analysis of a SoxB gene reveals neural

progenitor cells in the cnidarian *Nematostella vectensis*. Development 141, 4681–4689.
Richter, S., Loesel, R., Purschke, G., Schmidt-Rhaesa, A., Scholtz, G., Stach, T., Vogt, L., Wanninger, A., Brenneis, G., Doring, C., Faller, S., Fritsch, M., Grobe, P., Heuer, C. M., Kaul, S., Moller, O.S., Muller, C.H.G., Rieger, V., Rothe, B.H., Stegner, M.E.J., Harzsch, S., 2010. Invertebrate neurophylogeny: suggested terms and definitions for a neuroanatomical glossary. Front. Zool. 7, 29.
Röttinger, E., Dahlin, P., Martindale, M.Q., 2012. A framework for the establishment of a cnidarian gene regulatory network for "endomesoderm" specification: the inputs of ss-catenin/TCF signaling. PLoS Genet. 8, e1003164.
Ryan, J.F., Baxevanis, A.D., 2007. Hox, Wnt, and the evolution of the primary body axis: insights from the early-divergent phyla. Biol. Direct 2, 37.
Ryan, J.F., Pang, K., Schnitzler, C.E., Nguyen, A.D., Moreland, R.T., Simmons, D.K., Koch, B.J., Francis, W.R., Havlak, P., Program, N.C.S., Smith, S.A., Putnam, N.H., Haddock, S.H., Dunn, C.W., Wolfsberg, T.G., Mullikin, J.C., Martindale, M.Q., Baxevanis, A.D., 2013. The genome of the ctenophore *Mnemiopsis leidyi* and its implications for cell type evolution. Science 342, 1242592.
Safaiyan, F., Kolset, S.O., Prydz, K., Gottfridsson, E., Lindahl, U., Salmivirta, M., 1999. Selective effects of sodium chlorate treatment on the sulfation of heparan sulfate. J. Biol. Chem. 274, 36267–36273.
Sarrazin, S., Lamanna, W.C., Esko, J.D., 2011. Heparan sulfate proteoglycans. Cold Spring Harb. Perspect. Biol., 3. http://dx.doi.org/10.1101/cshperspect.a004952.
Sinigaglia, C., Busengdal, H., Leclère, L., Technau, U., Rentzsch, F., 2013. The bilaterian head patterning gene six3/6 controls aboral domain development in a cnidarian. PLoS Biol. 11, e1001488.
Sinigaglia, C., Busengdal, H., Lerner, A., Oliveri, P., Rentzsch, F., 2015. Molecular characterization of the apical organ of the anthozoan *Nematostella vectensis*. Dev. Biol. 398, 120–133.
Song, H.H., Shi, W., Xiang, Y.Y., Filmus, J., 2005. The loss of glypican-3 induces alterations in Wnt signaling. J. Biol. Chem. 280, 2116–2125.
Steinmetz, P.R., Urbach, R., Posnien, N., Eriksson, J., Kostyuchenko, R.P., Brena, C., Guy, K., Akam, M., Bucher, G., Arendt, D., 2010. Six3 demarcates the anterior-most developing brain region in bilaterian animals. EvoDevo 1, 14.
Thomas, J., Morle, L., Soulavie, F., Laurencon, A., Sagnol, S., Durand, B., 2010. Transcriptional control of genes involved in ciliogenesis: a first step in making cilia. Biol. Cell 102, 499–513.
Topczewski, J., Sepich, D.S., Myers, D.C., Walker, C., Amores, A., Lele, Z., Hammerschmidt, M., Postlethwait, J., Solnica-Krezel, L., 2001. The zebrafish glypican knypek controls cell polarity during gastrulation movements of convergent extension. Dev. Cell 1, 251–264.
Venero Galanternik, M., Kramer, K.L., Piotrowski, T., 2015. Heparan sulfate proteoglycans regulate Fgf signaling and cell polarity during collective cell migration. Cell Rep. 10, 414–428.
Veugelers, M., De Cat, B., Ceulemans, H., Bruystens, A.M., Coomans, C., Durr, J., Vermeesch, J., Marynen, P., David, G., 1999. Glypican-6, a new member of the glypican family of cell surface heparan sulfate proteoglycans. J. Biol. Chem. 274, 26968–26977.
Wang, S., Ai, X., Freeman, S.D., Pownall, M.E., Lu, Q., Kessler, D.S., Emerson Jr., C.P., 2004. Sulf1, a heparan sulfate 6-O-endosulfatase, inhibits fibroblast growth factor signaling in mesoderm induction and angiogenesis. Proc. Natl. Acad. Sci. USA 101, 4833–4838.
Wei, Z., Yaguchi, J., Yaguchi, S., Angerer, R.C., Angerer, L.M., 2009. The sea urchin animal pole domain is a Six3-dependent neurogenic patterning center. Development 136, 1179–1189.
Wikramanayake, A.H., Hong, M., Lee, P.N., Pang, K., Byrum, C.A., Bince, J.M., Xu, R., Martindale, M.Q., 2003. An ancient role for nuclear beta-catenin in the evolution of axial polarity and germ layer segregation. Nature 426, 446–450.
Yan, D., Wu, Y., Feng, Y., Lin, S.C., Lin, X., 2009. The core protein of glypican Dally-like determines its biphasic activity in wingless morphogen signaling. Dev. Cell 17, 470–481.
You, J., Belenkaya, T., Lin, X., 2011. Sulfated is a negative feedback regulator of wingless in Drosophila. Dev. Dyn. 240, 640–648.
Zhang, L., David, G., Esko, J.D., 1995. Repetitive Ser-Gly sequences enhance heparan sulfate assembly in proteoglycans. J. Biol. Chem. 270, 27127–27135.